

Adaptive Diffusion Regularization for Enhancement of Microcalcifications in Digital Breast Tomosynthesis (DBT) Reconstruction

Yao Lu^{1*}, Heang-Ping Chan¹, Jeffrey A. Fessler²,
Lubomir Hadjiiski¹, Jun Wei¹, and Mitchell M. Goodsitt¹

¹Department of Radiology, University of Michigan, Ann Arbor, MI
²EECS Department, University of Michigan, Ann Arbor, MI

ABSTRACT

Digital breast tomosynthesis (DBT) has been shown to increase mass detection. Detection of microcalcifications in DBT is challenging because of the small, subtle signals to be searched in the large breast volume and the noise in the reconstructed volume. We developed an adaptive diffusion (AD) regularization method that can differentially regularize noise and potential signal regions during reconstruction based on local contrast-to-noise ratio (CNR) information. This method adaptively applies different degrees of regularity to signal and noise regions, as guided by a CNR map for each DBT slice within the image volume, such that potential signals will be preserved while noise is suppressed. DBT scans of an American College of Radiology phantom and the breast of a subject with biopsy-proven calcifications were acquired with a GE prototype DBT system at 21 angles in 3° increments over a ±30° range. Simultaneous algebraic reconstruction technique (SART) was used for DBT reconstruction. The AD regularization method was compared to the non-convex total p-variation (TpV) method and SART with no regularization (NR) in terms of the CNR and the full width at half maximum (FWHM) of the central gray-level line profile in the focal plane of a calcification. The results demonstrated that the SART regularized by the AD method enhanced the CNR and preserved the sharpness of microcalcifications compared to reconstruction without regularization. The AD regularization was superior to the TpV method for subtle microcalcifications in terms of the CNR while the FWHM was comparable. The AD regularized reconstruction has the potential to improve the CNR of microcalcifications in DBT for human or machine detection.

Keywords: digital breast tomosynthesis (DBT), regularization method, simultaneous algebraic reconstruction technique (SART), microcalcification

1. INTRODUCTION

Digital breast tomosynthesis (DBT) is an emerging imaging technique that utilizes limited angle computed tomography technology to provide quasi-3D structural information for the detection and diagnosis of breast cancer. A small number of low-dose x-ray projections of the breast are acquired at different angles over a limited angular range^{1,2}. The total radiation dose of tomosynthesis is set to be comparable to that used in conventional two-view mammography. A set of tomosynthesized slices is reconstructed from the limited-angle projections. The low radiation dose used by DBT scan results in higher noise level in DBT projection images than that in full field digital mammography (FFDM). The noise in the projection views is propagated to the reconstruction volume because of the ill-posed linear system of DBT. The noise affects the visibility and detectability of subtle microcalcifications in DBT reconstruction images.

Simultaneous algebraic reconstruction technique (SART) is an iterative reconstruction method for DBT reconstruction^{3,4}. Previous studies have shown that SART is effective to obtain DBT reconstructions with good image quality in a few iterations³. The contrast of microcalcifications can be increased by increasing the number of iterations in SART. However, the image noise is amplified with an increasing number of iterations. Regularization method is an effective method widely used in image processing field to suppress image noise. Most existing regularization methods for DBT reconstruction are driven by local gradient^{5,6}. Because of their small size and low gradient, subtle

* email: yaol@med.umich.edu

microcalcifications might be treated as noise and smoothed out by the gradient-driven regularization methods. We are developing new regularization methods specifically designed for enhancing the contrast of subtle microcalcifications^{7,8}. In this study, we designed a regularized reconstruction method that can differentially regularize noise and potential signal regions during reconstruction based on local contrast-to-noise ratio (CNR) information. The performance of this method was compared with that of the non-convex total p-variation regularization method⁶ and reconstruction without regularization in terms of their capability of CNR enhancement and preservation of the sharpness of calcifications of various sizes.

2. METHODS AND MATERIALS

2.1 DBT System

A GE GEN2 prototype DBT mammography system with a stationary digital detector was used for acquisition of DBT scans of an American College of Radiology (ACR) mammography phantom and the breast of human subjects with biopsy-proven microcalcifications. Patient imaging was performed with IRB approval and informed consent. The DBT of a subject with a malignant cluster containing microcalcifications of various sizes and contrasts was chosen as an example in this study.

The imaging geometry of this DBT system is illustrated in Figure 1. The distance from x-ray focal spot to the center of the rotation is 64 cm and the x-ray source rotation plane is parallel to the chest wall. The system has a CsI phosphor/a:Si active matrix flat panel digital detector with a pixel pitch of 0.1 mm X 0.1 mm. The digital detector is stationary during image acquisition. The distance from the breast support plate, where the center of the x-ray source rotation is located, to the detector plane is 2 cm. The DBT system uses an Rh-target/Rh-filter x-ray source for all breast thicknesses. The system uses a step-and-shoot design and acquires 21 projection view images in 3° increments over a ±30° range in less than 8 seconds.

2.2 Reconstruction Method

Simultaneous algebraic reconstruction technique (SART) was used for DBT reconstruction in this study. SART is an iterative reconstruction algorithm which provides a successive approximation of a weighted least square solution of the DBT reconstruction problem. SART converges fast and the number of iterations affects image quality and computation cost. In our implementation, the voxel dimensions in the X and Y directions were both chosen to be 0.1 mm, matching the detector pixel size. The slice interval in the Z direction was chosen to be 1 mm. A ray-tracing algorithm similar to the Siddon algorithm is employed for calculating the contribution of each voxel to the forward projection⁹.

Let A_n denote the projection matrix for the n -th projection view ($1 \leq n \leq N$), where $A_n = (A_{ij,n})$ and $A_{ij,n}$ is the pathlength of the i -th ray from the x-ray source to the detector intersecting the j -th voxel in the reconstruction image volume in the n -th projection. To simplify our notations, we introduce two definitions, the row sum and column sum of the projection matrix A_n as

$$A_{i+,n} = \sum_{j=1}^J A_{ij,n} \quad \text{and} \quad A_{+j,n} = \sum_{i=1}^I A_{ij,n}.$$

In each SART iteration, the reconstructed image volume is updated view by view as follows:

$$x_j^{n,k} = x_j^{n-1,k} + \frac{\lambda}{A_{+j,n}} \sum_{i=1}^I \frac{A_{ij,n}}{A_{i+,n}} (y_{i,n} - (A_n x^{n-1,k})_i)$$

for $1 \leq j \leq J$, where J is the number of voxels in the reconstruction image volume, $1 \leq i \leq I$, I is the number of detector pixels, k is the index of the iteration, $y_{i,n}$ is the i -th pixel of the n -th projection view and $x_j^{n,k}$ is the linear attenuation coefficient of the j -th voxel after the n -th projection view updated sequentially in the k -th iteration. The relaxation parameters λ were set to be 0.5 in the first iteration and 0.3 in the subsequent iterations. We previously showed that SART without regularization can enhance the contrast and edges of high-contrast features but simultaneously amplify the image noise. Therefore, regularization method that suppresses noise and preserves image features is needed to improve the image quality of DBT reconstruction.

2.3 Adaptive Diffusion Regularization

Several regularization methods have been studied in the context of DBT reconstruction.^{5-8, 10} Most existing regularization methods are driven by local gradient. Pixels with small gradient may be treated as noise and smoothed out. The main challenge of implementing regularization in DBT reconstruction is to differentiate subtle microcalcifications from the noisy background such that microcalcifications will be preserved while noise is suppressed. In this study, we designed a new adaptive diffusion (AD) regularization method that selectively applies different degrees of regularization to background and potential signal locations for SART, as guided by a contrast-to-noise ratio (CNR) map generated for each reconstructed slice from the previous iteration.

To generate the CNR map for a given slice, the low-frequency background of the DBT slice is first removed from the image. High-contrast locations are identified by an iterative global thresholding method. At each high-contrast location, local CNR analysis is performed and the pixels above a threshold CNR are labeled. The collection of high CNR locations over the entire DBT slice constitutes the CNR map of this slice. Such CNR maps are generated for all slices throughout the DBT volume. The CNR maps mark the location of potential signal regions and are then used to guide regularization over the whole image volume for reconstruction during updating with each projection view in the next iteration of SART. For a given image v , we denote $S(v)$ the CNR map generated from v . $S(v)$ is a binary matrix, in which the elements indicating potential signal regions have value 1 and otherwise 0.

We denote ∇ the gradient operator. A function $c(u, v)$ is used to guide the degree of regularization applied to u according to the CNR map v . Using the regularized SART, after all rays in one projection view have been processed once, the linear attenuation coefficient of each voxel will be updated by

$$x_j^{n,k} = x_j^{n-1,k} + \frac{\lambda}{A_{+,j,n}} \sum_{i=1}^I \frac{A_{ij,n}}{A_{i+,n}} (y_{i,n} - (A_n x^{n-1,k})_i + \mu c(x^{n-1,k}, S(x^{0,k}))),$$

for $1 \leq j \leq J$, where μ is the regularization parameter and the function $c(u, v)$ is defined as

$$c(u, v) = v \circ (\nabla \cdot (\nabla u)),$$

and \circ denote the Hadamard (entrywise) product of two matrices with the same dimension. $x^{0,k}$ is the image volume input to the k -th iteration for $k > 1$, no regularization is applied when $k=1$.

2.4 Figure-of-Merit

To evaluate the effect of the proposed regularization method on MC enhancement and noise suppression, the CNR of selected signals and the full width at half maximum (FWHM) of selected line profiles across signals in the reconstructed DBT images will be measured for both a breast phantom and a human subject.

The normalized line profile and its FWHM in the focal plane of a calcification were used to measure the in-plane image sharpness. The baseline of each line profile was calculated from the average of the background pixels in the neighborhood of the object of interest and subtracted from the line profile. A Gaussian function was used for curve fitting of the background-corrected linear profile, and the FWHM of the line profile was computed as

$$FWHM = (2\sqrt{2\ln 2})\sigma$$

where σ is the standard deviation of the fitted Gaussian function.

The CNR value of the selected signal region of interest (ROI) was used to measure the contrast relative to the background noise of the signal of interest. The CNR value is defined by

$$CNR = \frac{\bar{I}_{ROI} - \bar{I}_{BG}}{\sigma_{BG}}$$

where \bar{I}_{ROI} is the mean pixel value in a selected ROI centered around the same pixel location as the center of the calcification, \bar{I}_{BG} is the mean pixel value in an ROI of a neighboring background region located at the same slice, and σ_{BG} is the standard deviation of pixel values in the background ROI. All measurements were obtained by averaging the results from six repeated DBT scans of the same phantom under the same imaging conditions.

3. RESULTS

The AD regularization method was applied to six repeated DBT scans of the ACR mammography accreditation phantom and the DBT scan of the selected human subject. The AD regularization was compared with the non-convex total p-variation (TpV) regularization method⁶ and SART with no regularization (NR). The comparisons were performed over five iterations of SART and the results after the fifth iteration were discussed below.

Four simulated calcifications with various nominal diameters (0.54 mm, 0.32 mm, 0.24 mm and 0.24 mm) were selected from the reconstructed ACR phantom images. The in-focus DBT slice of the simulated microcalcification clusters of the ACR phantom reconstructed with no regularization is displayed in Figure 2. A comparison of the CNR values of the selected signals in phantom DBT for the three methods is shown in Figure 3. The AD method provided the highest CNR value among the three methods for all four signals. The FWHM values of the selected central gray-level line profiles in the phantom DBT are plotted in Figure 4. It can be seen that the trends of FWHM values are consistent between the x- and y- directions. For large microcalcifications, the TpV method had smaller FWHM values than the AD and NR methods while the AD method was comparable to the NR method, indicating that the AD method could preserve the shapes of signals. For small signals, the standard deviations of the measurements were large and all methods were comparable within the measurement error.

Three calcifications with various sizes were selected from one cluster (Fig. 5 (a)) of the DBT of the human subject for analysis. The in-focus DBT slice of the human subject microcalcification clusters reconstructed with different regularization methods are compared in Figure 5. Visual comparison indicates that both the TpV and the AD method significantly reduced the noise level. The TpV method suffers from the staircasing effect, the piecewise constant background artifact at the left upper corner of Fig. 5(b). The AD method improved the conspicuity of the whole microcalcification cluster, including the subtle microcalcifications. The AD method avoided the *staircasing* effect and provided higher contrast for subtle microcalcifications than the TpV and the NR methods; whereas, the TpV method appears to have sharper microcalcifications than the other methods. The shape of the signals in DBT reconstruction using the AD method was visually similar to that using the NR method. Figure 6 confirms that, in terms of the CNR value, the AD method was comparable to the TpV method for large microcalcifications and superior for subtle microcalcifications. The FWHM values of the selected central gray-level line profiles across the signals are compared in Figure 7. There are variations in the relative trends of the FWHM values of the signals of different sizes, although the FWHM values of the AD method appear to be more similar than those of the TpV method in comparison to NR. The varied trends may be attributed to the large uncertainties in these single measurements.

4. DISCUSSION AND CONCLUSIONS

The adaptive diffusion regularization method applies regularization with different degrees of regularity guided by the CNR maps within the image volume. The adaptive diffusion regularization method exploits neighboring information of the voxels to characterize potential signal region. It is effective in suppressing noise, reducing *staircasing* effect and enhancing the visibility of microcalcifications. The effect of regularization on signal quality was evaluated quantitatively using DBT data of an ACR phantom and a patient breast. The results demonstrate that the SART regularized by the adaptive diffusion method enhanced the CNR and preserved the sharpness of microcalcifications. The AD regularization was superior to the TpV method for subtle microcalcifications. The AD regularized reconstruction has the potential to improve the CNR of microcalcifications in DBT for human or machine detection.

ACKNOWLEDGMENTS

This work is supported by USPHS grants R33 CA120234 and R01 CA91713. The digital breast tomosynthesis system was developed by the GE Global Research Group through the Biomedical Research Partnership (USPHS grant CA91713, PI: Paul Carson, Ph.D.) collaboration. The content of this paper does not necessarily reflect the position of the funding agencies and no official endorsement of any equipment and product of any companies mentioned should be inferred.

REFERENCES

- [1] Niklason, L. T., Christian, B. T., Niklason, L. E., Kopans, D. B., Castleberry, D. E., Opsahl-Ong, B. H., Landberg, C. E., Slanetz, P. J., Giardino, A. A., Moore, R., Albagli, D., Dejule, M. C., Fitzgerald, F. C., Fobare, D. F., Giambattista, B. W., Kwasnick, R. F., Liu, J., Lubowski, S. J., Possin, G. E., Richotte, J. F., Wei, C. Y. and

- Wirth, R. F., "Digital tomosynthesis in breast imaging," *Radiology* 205, 399-406 (1997).
- [2] Wu, T., Stewart, A., Stanton, M., Mccauley, T., Phillips, W., Kopans, D. B., Moore, R. H., Eberhard, J. W., Opsahl-Ong, B., Niklason, L. and Williams, M. B., "Tomographic mammography using a limited number of low-dose cone-beam projection images," *Medical Physics* 30, 365-380 (2003).
- [3] Zhang, Y., Chan, H.-P., Sahiner, B., Wei, J., Goodsitt, M. M., Hadjiiski, L. M., Ge, J. and Zhou, C., "A comparative study of limited-angle cone-beam reconstruction methods for breast tomosynthesis," *Medical Physics* 33, 3781-3795 (2006).
- [4] Han, T., Zhong, Y., Chen, L., Lai, C., Liu, X., Shen, Y., Ge, S., Yi, Y. and Shaw, C., "Su-ff-i-41: Accuracy and computing time of a ray-driven projector/back-projector for simulation and reconstruction in tomosynthesis and cone beam ct imaging," *Medical Physics* 36, 2443-2444 (2009).
- [5] Sidky, E. Y., Reiser, I. S., Nishikawa, R. and Pan, X. C., "Image reconstruction in digital breast tomosynthesis by total variation minimization," *Proc of SPIE* 6510, 651027 (2007).
- [6] Sidky, E. Y., Pan, X., Reiser, I., Nishikawa, R. M., Moore, R. H. and Kopans, D. B., "Enhanced imaging of microcalcifications in digital breast tomosynthesis through improved image-reconstruction algorithms," *Medical Physics* 36, 4920-4932 (2009).
- [7] Lu, Y., Chan, H. P., Goodsitt, M. M., Wei, J., Hadjiiski, L. and Schmitz, A., "Enhancement of microcalcifications in digital breast tomosynthesis (DBT): Effects of contrast-enhancing regularization," *RSNA Program Book 2010, SSJ24* (2010).
- [8] Lu, Y., Chan, H. P., Wei, J. and Hadjiiski, L. M., "Selective-diffusion regularization for enhancement of microcalcifications in digital breast tomosynthesis reconstruction," *Medical Physics* 37, 6003-6014 (2010).
- [9] Siddon, R. L., "Fast calculation of the exact radiological path for a three-dimensional CT array," *Medical Physics* 12, 252-255 (1985).
- [10] Sidky, E. Y., Reiser, I., Nishikawa, R. M., Pan, X. C., Chartrand, R., Kopans, D. B. and Moore, R. H., "Practical iterative image reconstruction in digital breast tomosynthesis by non-convex TpV optimization," *Proc of SPIE* 6913, 91328 (2008).

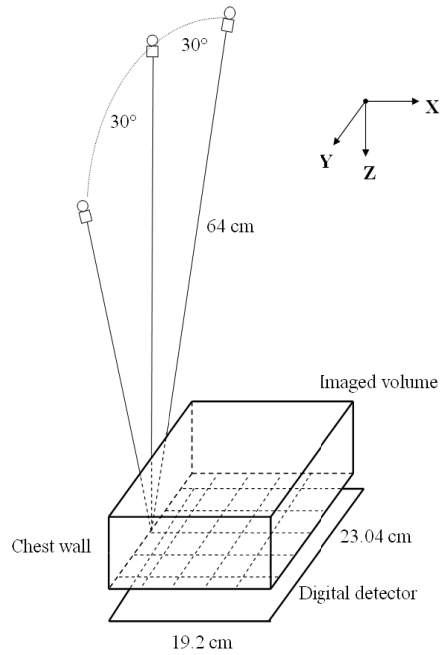


Figure 1. Geometry of the GE prototype GEN2 digital breast tomosynthesis system used in this study.

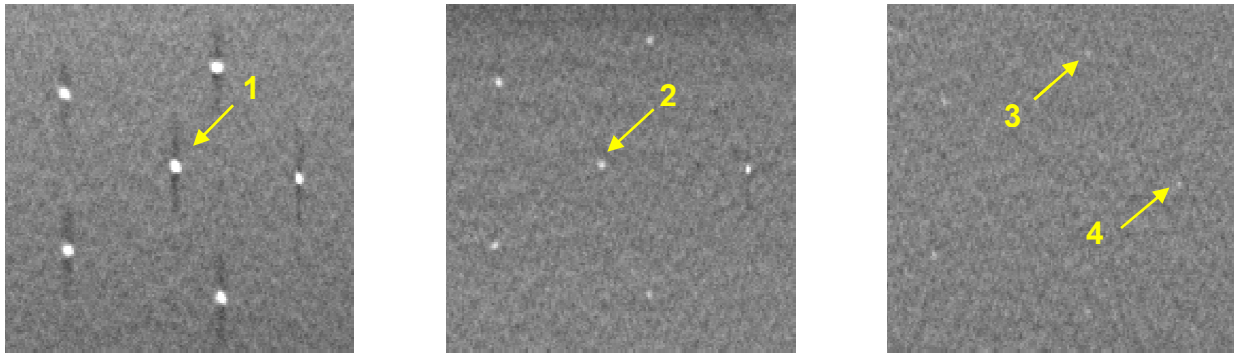


Figure 2. Regions of interest from a DBT slice of the ACR phantom reconstructed without regularization showing the largest, the third, and the fourth speck groups. The signals 1, 2, 3 and 4, with nominal size of 0.54 mm, 0.32 mm, 0.24 mm and 0.24 mm, respectively, were selected for analysis in this study.

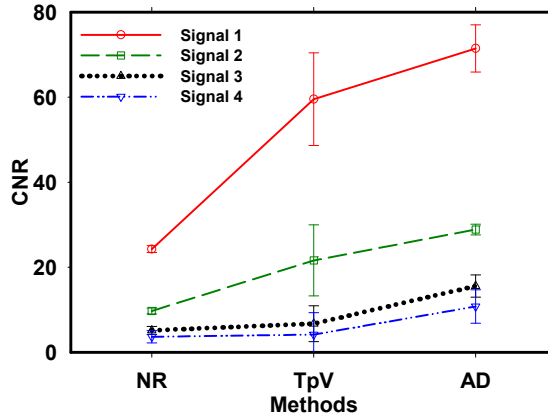


Figure 3. The CNRs for 4 simulated calcifications in the reconstructed ACR phantom images. The error bars indicate \pm one standard deviation estimated from the six repeated measurements. The nominal sizes of the signals are 0.54 mm (signal 1), 0.32 mm (signal 2) and 0.24 mm (signal 3 and 4), respectively. The AD method provides the highest CNR value among the three methods. For the subtle signals (signal 3 and signal 4), the AD method provided more than 100% higher CNR than the other two methods.

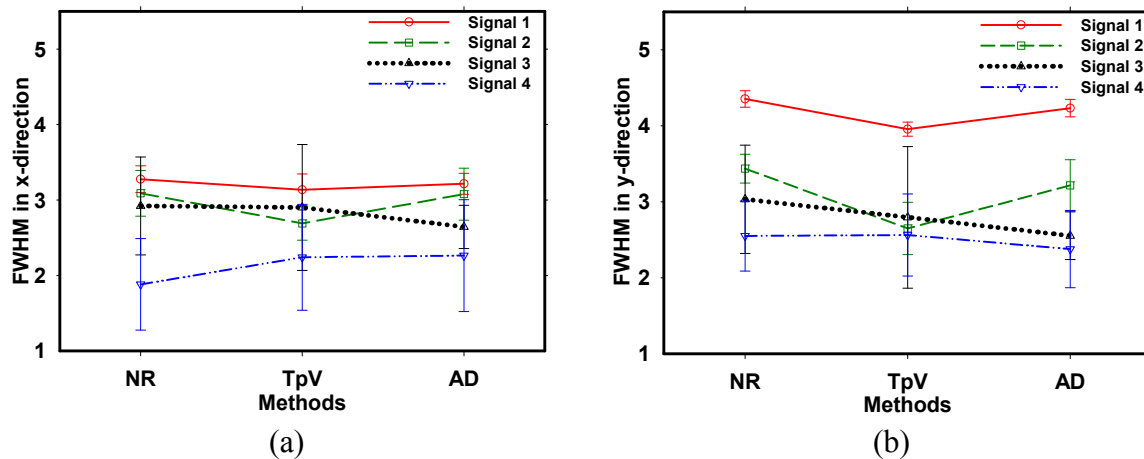


Figure 4. Comparison of FWHM values for the two regularization methods and without regularization in the (a) x-direction and (b) y-direction. The FWHM values were measured for the four simulated microcalcifications selected from the ACR phantom. All values were obtained by averaging six repeated measurements. The error bars indicate \pm one standard deviation estimated from the six repeated measurements. For large signals (signal 1 and 2), the TpV methods had smaller FWHM values than the other methods while the AD method was comparable to NR, indicating that the AD method could preserve the shapes of signals. For small signals (signal 3 and 4), the standard deviations of the measurements were large and all methods were comparable within the measurement error.

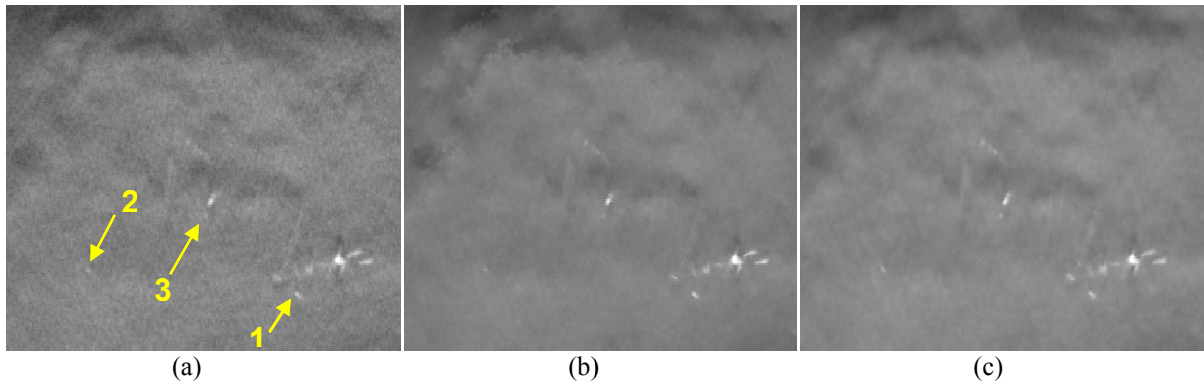


Figure 5. Comparison of the in-focus DBT slice for three selected calcifications in the DBT of a human subject for the three methods. The three selected signals were numbered in approximately decreasing size and contrast. The DBT was reconstructed by SART with five iterations: (a) without regularization (NR), (b) with non-convex total p-variation (TpV) regularization, and (c) with the new adaptive diffusion (AD) regularization. All images were displayed with the same window and level settings.

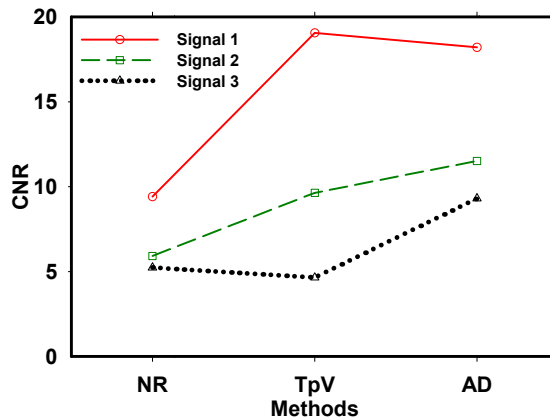


Figure 6. Comparison of the CNR values of calcifications of various sizes from a DBT scan of a human subject reconstructed with two regularization methods and without regularization. DBT reconstructed by SART with five iterations were compared. The TpV method obtained the highest CNR for signal 1 (large size). For signal 3 (small size), the AD method achieved 80-100% higher CNR than the other two methods.

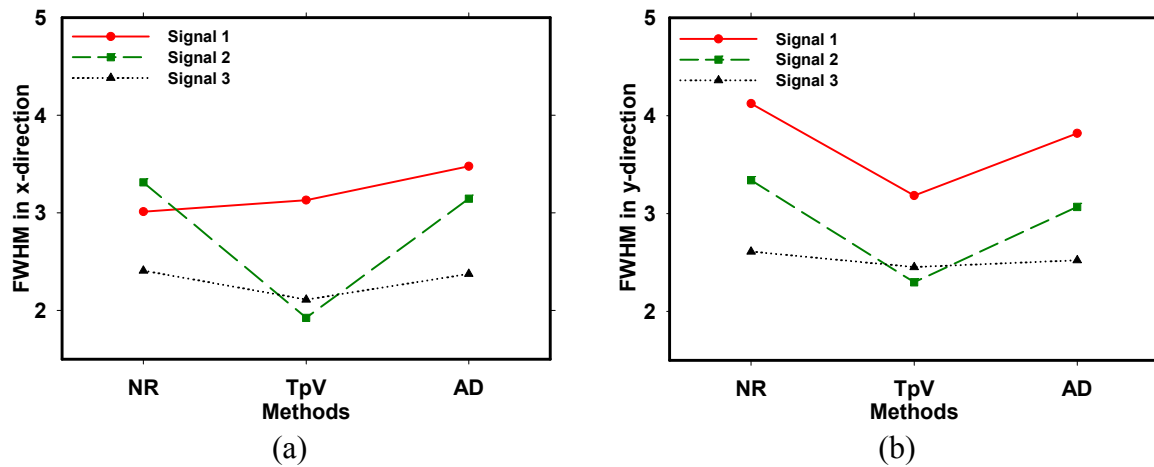


Figure 7. Comparison of FWHM values for the two regularization methods and without regularization in the (a) x-direction and (b) y-direction. FWHM values were measured for the three microcalcifications selected from the DBT of a human subject. The relative trends of the three methods varied, probably because of the large uncertainties in these single measurements.